J. CHEM. SOC. FARADAY TRANS., 1991, 87(3), 473–478

Kinetics of Corrosion of Ruthenium Dioxide Hydrate by Ce^{IV} Ions

Andrew Mills* and Hefin Davies
Department of Chemistry, University College of Swansea, Singleton Park, Swansea SA2 8PP, UK

The kinetics of oxidative dissolution of $RuO_2 \cdot xH_2O$ to RuO_4 by Ce^{IV} ions are studied. Under conditions of a low $[Ce^{IV}] : [RuO_2 \cdot xH_2O]$ ratio (*e.g.* 0.35 : 1) and a high background concentration of Ce^{III} ions (which impede dissolution) the initial reduction of Ce^{IV} ions is due to charging of the $RuO_2 \cdot xH_2O$ microelectrode particles. The initial rate of charging depends directly upon $[RuO_2 \cdot xH_2O]$ and has an activation energy of 25 ± 5 kJ mol^{-1}. Under conditions of a high $[Ce^{IV}] : [RuO_2 \cdot xH_2O]$ (*e.g.* 9 : 1) and a low background $[Ce^{III}]$ the reduction of Ce^{IV} ions is almost totally associated with the dissolution of $RuO_2 \cdot xH_2O$ to RuO_4, *i.e.* not charging. The kinetics of dissolution obey an electrochemical model in which the reduction of Ce^{IV} ions and the oxidation of $RuO_2 \cdot xH_2O$ to RuO_4 are assumed to be highly reversible and irreversible processes, respectively, mediated by dissolving the microelectrode particles of $RuO_2 \cdot xH_2O$. Asssuming this electrochemical model, from an analysis of the kinetics of dissolution the activation energy for this process was estimated to be 39 ± 5 kJ mol^{-1} and the Tafel slope for $RuO_2 \cdot xH_2O$ corrosion was calculated to be 15 mV per decade. The mechanistic implications of these results are discussed.

The oxides of ruthenium(IV) containing little or no water of hydration are known to be excellent stable electrocatalysts for the oxidation of water to oxygen, or brine to chlorine.[1] In contrast, when highly hydrated ruthenium dioxide (H_2O content ≈24%) is used as an anode for the oxidation of water the main electro-oxidation reaction which occurs is the dissolution of the anode to ruthenium tetroxide,[2,3] RuO_4. Similar conclusions have been reached in studies[4] on the abilities of these same oxides (as powders, dispersed in solution) to act as redox catalysts for the oxidation of water by Ce^{IV} ions and other strong oxidants, *i.e.*

$$4Ce^{IV} + 2H_2O \xrightarrow[\text{catalyst}]{\text{redox}} 4Ce^{III} + 4H^+ + O_2 \qquad (1)$$

Extensive work[5] has established that there is an optimum form of partially dehydrated ruthenium dioxide for catalysing reaction (1) with an H_2O content of *ca.* 10%. Although samples of ruthenium dioxide hydrate with a lower H_2O content are very stable towards corrosion to RuO_4 by Ce^{IV} ions, they usually have a lower surface area, *i.e.* the surface area of powdered ruthenium dioxide hydrate decreases with decreasing H_2O content, and, thus, are less active per gram of catalyst. In contrast, samples of ruthenium dioxide hydrate with an H_2O content >10% have a higher surface area than the optimum sample, but they also tend to undergo an oxidative dissolution reaction which increases with increasing H_2O content.[6] Thus, using highly hydrated ruthenium dioxide, $RuO_2 \cdot xH_2O$, with an H_2O content of *ca.* 24%, the reaction is almost completely corrosion rather than O_2 catalysis. For $RuO_2 \cdot xH_2O$ we have established[6] that the overall corrosion reaction comprises two simultaneous processes, *i.e.*

$$4Ce^{IV} + RuO_2 \cdot xH_2O + 2H_2O \rightarrow 4Ce^{IIII} + RuO_4 + xH_2O + 4H^+ \qquad (2a)$$

and

$$4zCe^{IV} + 2zH_2O \rightarrow 4zCe^{III} + 4zH^+ + zO_2 \qquad (2b)$$

where $z \approx 0.26$. In our initial work[6] we suggested that the source of the water oxidised in reaction (2*b*) originated from the hydrate itself, rather than the solvent. However, the results of a more recent study by our group[7] using O^{18}-labelled water in the solvent and mass spectrometry for gas analysis, indicate that the O_2 generated *via* reaction (2*b*) comes from the solvent.

In the few studies of the kinetics of redox-catalysed oxygen evolution, *via* reactions such as (1), the results have been rationalised successfully using an electrochemical model in which the redox catalyst particles act as microelectrodes.[4] This electrochemical approach to explaining what happens when two, or more, redox couples are present together but not in equilibrium, has found extensive use in characterising many corrosion reactions involving the dissolution of a metal, alloy or metal oxide, by a homogeneous redox couple, *e.g.* the corrosion of iron or stainless steel by acid.[8,9]

So far, most of these corrosion studies have concentrated on the dissolution of such materials in macroelectrode form, since it is a relatively simple task to determine the necessary current *vs.* voltage curves for the two redox couples involved as well as to determine the rate of corrosion of the macroelectrode and its mixture potential and so show whether the electrochemical model is appropriate or not. Interestingly, there appears to be little, if any, work on the dissolution of materials in micro- rather than macroelectrode form, *i.e.* as particles dispersed in solution rather than as bulk electrodes. This is surprising given the relevance of such work to mineralogy, hydrometallurgy and nuclear-plant decontamination.[10]

In a previous paper[11] we demonstrated that the kinetics of the oxidation of water by Ce^{IV} ions [reaction (1)] mediated by thermally activated (*i.e.* partially dehydrated) ruthenium dioxide hydrate can be readily explained using an electrochemical model[12] of redox catalysis in which the reduction of Ce^{IV} ions and oxidation of water are considered as highly reversible and irreversible reactions, respectively. In this paper we investigate the kinetics of oxidative dissolution of fully hydrated ruthenium dioxide hydrate, $RuO_2 \cdot xH_2O$, by Ce^{IV} ions to see if, as might be expected, they fit a similar electrochemical model, where the reduction of Ce^{IV} ions is again considered to be a highly reversible process and the oxidation of $RuO_2 \cdot xH_2O$ to RuO_4 a highly irreversible reaction.

Experimental

Materials

The highly hydrated (24% H_2O content) sample of $RuO_2 \cdot xH_2O$ used throughout this work was obtained from Johnson Matthey (batch no. 065154A). The $RuO_2 \cdot xH_2O$ was used to make a stock dispersion in 0.5 mol dm^{-3} H_2SO_4 (usually 100 or 51 mg dm^{-3}), the preparation and handling of which has been described in detail elsewhere.[11] All Ce^{IV} solutions were prepared from an analytical volumetric 0.1 mol dm^{-3} Ce^{IV} sulphate solution using 0.5 mol dm^{-3} H_2SO_4 (AnalaR) as the diluent. A 0.1 mol dm^{-3} Ce^{III} sulphate stock solution was prepared by reduction of the 0.1 mol dm^{-3} Ce^{IV} solution with a small excess of non-stabilised hydrogen peroxide, any residual of which was destroyed by refluxing the solution for 4 h. Subsequent dilutions were made with 0.5 mol dm^{-3} H_2SO_4. Unless stated otherwise, all chemicals were purchased from BDH, and the water used was doubly distilled and deionised.

Methods

The kinetics of dissolution of $RuO_2 \cdot xH_2O$ were monitored spectrophotometrically *via* the disappearance of the Ce^{IV} ions at $\lambda = 430$ nm [$\varepsilon(Ce^{IV})_{430} = 290$ dm^3 mol^{-1} cm^{-1}]. All kinetic runs were carried out in a fluorescence cell containing a Teflon stirrer bar rotating at a fixed rate (*ca.* 1100 rpm). In this cell were placed 2.5 cm^3 of a stock $RuO_2 \cdot xH_2O$ dispersion (the concentration of which was usually 51 or 100 mg dm^{-3}) and, in some cases, an aliquot of a Ce^{III} solution of known concentration. The dissolution reaction was initiated with the injection of a small amount (typically 90 mm^3) of a Ce^{IV} solution of known concentration (typically 0.01–0.1 mol dm^{-3}). The subsequent change of absorbance *vs.* time was monitored using a Perkin-Elmer Lambda 3 spectrophotometer and recorded and stored using a microcomputer (BBC Masterclass). Derivative versions of the absorbance *vs.* time plots were calculated from the original data using the same microcomputer. Note at this point that technically the derivative versions of the absorbance *vs.* time plots comprise a component due to the Ce^{IV} ions and one due to the $RuO_2 \cdot xH_2O$ particles dispersed in solution. However, the absorption spectrum of the powder dispersion alone is weak, flat and featureless and, as a result, the component due to the particle dispersion in any derivative plot is negligible. This last point was confirmed by monitoring the change in absorbance as a function of time as dissolution proceeds at a wavelength where only the dispersion (not Ce^{IV}) absorbs, *i.e.* at 700 nm in our work.

Results and Discussion

Experiments using an Excess of $RuO_2 \cdot xH_2O$

It seems reasonable to assume that the dissolution of $RuO_2 \cdot xH_2O$ by Ce^{IV} ions will be like most other dissolution reactions[10] in that the rate of dissolution will be proportional to the instantaneous surface area (of the $RuO_2 \cdot xH_2O$ particles, in this case). Thus, if the concentration of Ce^{IV} ions is in vast excess compared with the concentration of $RuO_2 \cdot xH_2O$, analysis of the kinetics of dissolution will be complicated by the fact that the rate of dissolution will decrease as the reaction proceeds since, as the particles dissolve the instantaneous surface area will itself decrease concomitantly. This problem can be overcome by having the opposite situation, *i.e.* a significant excess of $RuO_2 \cdot xH_2O$ compared with $[Ce^{IV}]$, since under these conditions the surface area will be approximately constant as the reduction of Ce^{IV} ions proceeds. In practice, the concentration of $RuO_2 \cdot xH_2O$ cannot be made too large since it is a black powder and at concentrations of 400 mg dm^{-3} the absorbance of the solution is >2 (in a 1 cm cell) at all wavelengths, which makes the spectrophotometric monitoring of $[Ce^{IV}]$ decay as a function of time (after injection) unreliable.

In these experiments, therefore, we used a 100 mg dm^{-3} $RuO_2 \cdot xH_2O$ solution (0.56 mmol dm^{-3}) which had an absorbance at 430 nm of *ca.* 0.5. In order to have an excess of $RuO_2 \cdot xH_2O$ over Ce^{IV} ions, assuming a 4 : 1 Ce^{IV} : $RuO_2 \cdot xH_2O$ reaction stoichiometry, 50 mm^3 of a 0.01 mol dm^{-3} Ce^{IV} solution were injected into the $RuO_2 \cdot xH_2O$ dispersion, giving a final $[Ce^{IV}]$ of 0.2 mmol dm^{-3}, *i.e.* an 11-fold excess of $RuO_2 \cdot xH_2O$ over Ce^{IV} after injection and mixing. Typical absorbance *vs.* time profiles under these reaction conditions, without and with a high concentration of Ce^{III} ions (7.4×10^{-2} mol dm^{-3}), are illustrated in Fig. 1(*a*) and (*b*), respectively. From the data illustrated in Fig. 1, the Ce^{IV} decay appears to have two distinct steps, a rapid initial decay which is insensitive to the presence of Ce^{III} ions and a slower subsequent process which is greatly impeded by Ce^{III} ions. Previous work by our group has established[6] that dissolution of $RuO_2 \cdot xH_2O$ by Ce^{IV} ions is almost totally prevented if a high concentration of Ce^{III} ions is present. Thus, from the data illustrated in Fig. 1 it appears that before dissolution there is a significant initial reaction involving the reduction of Ce^{IV} ions which is largely unimpeded by the presence of Ce^{III} ions. Experiments with an oxygen electrode showed that no oxygen was generated during any part of these runs.

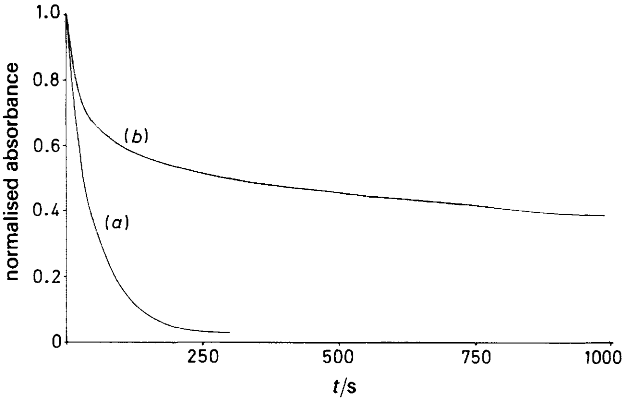

Fig. 1 Relative absorbance *vs.* time profiles recorded at 430 nm for the decay of a sample of Ce^{IV} ions (50 mm^3, 0.01 mol dm^{-3}, 0.5 mol dm^{-3} H_2SO_4) injected into 2.5 cm^3 of a $RuO_2 \cdot xH_2O$ dispersion (100 mg dm^{-3}) in 0.5 mol dm^{-3} H_2SO_4 without (*a*) or with (*b*) a high concentration of Ce^{III} ions (0.074 mol dm^{-3})

A number of experiments were carried out to determine the degree of corrosion of $RuO_2 \cdot xH_2O$ to RuO_4 by Ce^{IV} under the conditions of excess of $RuO_2 \cdot xH_2O$ and low $[Ce^{IV}]$ described above and without a high background concentration of Ce^{III} ions. In several of these experiments a flow system was used[6] in which 20 mg of $RuO_2 \cdot xH_2O$ were dispersed in 100 cm^3 of 0.5 mol dm^{-3} H_2SO_4 and placed into a 100 cm^3 Dreschel bottle. A continuous flow of nitrogen through this reaction vessel was used to sweep out any RuO_4 produced which was then trapped out as perruthenate using 20 cm^3 of solution containing 0.1 mol dm^{-3} NaOCl in 1 mol dm^{-3} NaOH in a second Dreschel bottle. The amount of RuO_4 trapped was determined spectrophotometrically. These experiments appeared to show that with an injection of 4×10^{-5} mol of Ce^{IV} ions (*i.e.* 4 cm^3 of a 0.01 mol dm^{-3} Ce^{IV} solution) no RuO_4 is produced, even in the absence of an excess of Ce^{III} ions. However, blank experiments using injections of the amount of RuO_4 expected (*i.e.* 10^{-5} mol) demonstrated that in the presence of a high concentration of $RuO_2 \cdot xH_2O$ most of the RuO_4 present in the reaction vessel is not swept out to the trap but rather decomposes *via* the following reaction:

$$RuO_4 \xrightarrow[\text{catalyst}]{RuO_2 \cdot xH_2O} RuO_2 + O_2 \qquad (3)$$

Unfortunately, the flow system removes any RuO_4 present in the reaction vessel too slowly (it takes *ca.* 7 h to strip all the RuO_4 from the reaction vessel to the trap by this method) to prevent its substantial decomposition *via* reaction (3). However, an alternative system was devised in which any RuO_4 present in the reaction vessel was removed very rapidly into a layer of carbon tetrachloride placed in contact with the reaction solution. The partition coefficient for RuO_4 between water and CCl_4 is *ca.* 1/50 and thus in our biphasic system the RuO_4 can be stripped almost quantitatively from an aqueous solution using CCl_4 and then analysed spectrophotometrically.[13] In these experiments washed CCl_4 (10 cm^3) was placed in contact with the reaction solution (25 cm^3 of 0.5 mol dm^{-3} H_2SO_4 containing 10 mg of $RuO_2 \cdot xH_2O$) into which was injected 2 cm^3 of a 0.01 mol dm^{-3} Ce^{IV} solution, however, no RuO_4 was detected even though blank experiments showed that the collection efficiency of the CCl_4 layer was 100% in the presence and absence of a high concentration of $RuO_2 \cdot xH_2O$ [*i.e.* reaction (3) was not responsible for the lack of RuO_4 detected].

From the results of this work it appears that under the conditions of these initial experiments, *i.e.* high [$RuO_2 \cdot xH_2O$] and low [Ce^{IV}], the observed reduction of Ce^{IV} ions is not associated with either reactions (2*a*) or (2*b*) but rather some other process. One of the simplest explanations is that the Ce^{IV} ions are reduced by some impurity associated with the $RuO_2 \cdot xH_2O$. However, an alternative explanation, which also fits in with the electrochemical model of corrosion, is that before corrosion the particles of $RuO_2 \cdot xH_2O$ must be charged up by the Ce^{IV} ions.[14,15] The effect would be the reduction of Ce^{IV} ions without any apparent products such as O_2 or RuO_4. The process of charging may be represented by the general equation:

$$Ce^{IV} + (RuO_2 \cdot xH_2O)^{z+} \rightarrow Ce^{III} + (RuO_2 \cdot xH_2O)^{(z+1)+} \quad (4)$$

where $z+$ is the charge on the $RuO_2 \cdot xH_2O$ particle arising from other previous charging reactions. The process of charging should effectively continue until the rate of charging is equal to the rate of particle discharge by, say, the oxidation of Ce^{III} ions or surface Ru^{IV} species (leading to particle dissolution). Even if the corrosion process is greatly inhibited by the presence of a large excess of Ce^{III} ions some charging should still occur, albeit to a lesser extent.[14]

An interesting prediction of the above 'charging' model is that it should be possible to discharge 'charged' particles by adding to the dispersion an easily reduced species. If the reducing agent used is a redox indicator, like ferroin [1,10-phenanthroline iron(II) sulphate complex, $E^0 = 1.08$ V *vs.* HNE] for example, then the discharge of the $RuO_2 \cdot xH_2O$ particles by the reducing agent/redox indicator will be made apparent by a concomitant change in colour of the latter.

In a set of experiments to illustrate this point a solution of ferroin (80 mm^3, 0.005 mol dm^{-3}) was added to 2.5 cm^3 of 0.5 mol dm^{-3} H_2SO_4 solution containing either: (*a*) an uncharged dispersion of $RuO_2 \cdot xH_2O$ (100 mg dm^{-3}), (*b*) 40 mm^3 of a 0.01 mol dm^{-3} Ce^{IV} solution or (*c*) a 'charged' dispersion of $RuO_2 \cdot xH_2O$ (100 mg dm^{-3}). [The 'charged' dispersion of $RuO_2 \cdot xH_2O$ was prepared by injecting 40 mm^3 of a 0.01 mol dm^{-3} Ce^{IV} solution into solution (*a*) and leaving the solution until $\leqslant 1\%$ of the initial concentration of Ce^{IV} ions was present (*ca.* 500 s)]. Fig. 2 illustrates the absorption spectra of the final solutions [(*a*)–(*c*)]. The 1,10-phenanthroline iron(II) complex is red [λ(max) = 470 nm] and turns blue when oxidised by Ce^{IV} ions, for example. The same absorption spectrum as illustrated in Fig. 2(*a*) was obtained when just ferroin was injected into 0.5 mol dm^{-3} H_2SO_4 and is characteristic of the unoxidised form of this redox indicator. The experiment which generates the absorption spectrum in Fig. 2(*a*) demonstrates that the uncharged $RuO_2 \cdot xH_2O$ dispersion is not able to oxidise the ferroin redox indicator. The second absorption spectrum [Fig. 2(*b*)] illustrates that Ce^{IV} ions are able to oxidise ferroin in homogeneous solution, as might be expected given the high formal oxidation potential of the Ce^{IV}/Ce^{III} couple [*i.e.* $E^0 = 1.44$ V *vs.* NHE (0.5 mol dm^{-3} H_2SO_4)]. Most intriguing, however, is the absorption spectrum in Fig. 2(*c*) in which it appears that associated with the charged dispersion is *ca.* 80% of the number of oxidising equivalents as in the original Ce^{IV} solution used to charge it up [see Fig. 2(*b*)]. These oxidising equivalents are associated with the particles and not the solution, since, by the time the ferroin was added, the bulk [Ce^{IV}] in the charged dispersion was $\leqslant 1\%$ of that used to generate the absorption spectrum in Fig. 2(*b*). In addition, filtration to remove the charged particles and subsequent addition of ferroin to the filtrate generated the same absorption spectrum as illustrated in Fig. 2(*a*), indicating that there are no oxidising equivalents associated with the filtrate and, therefore, with the aqueous phase of the charged dispersion.

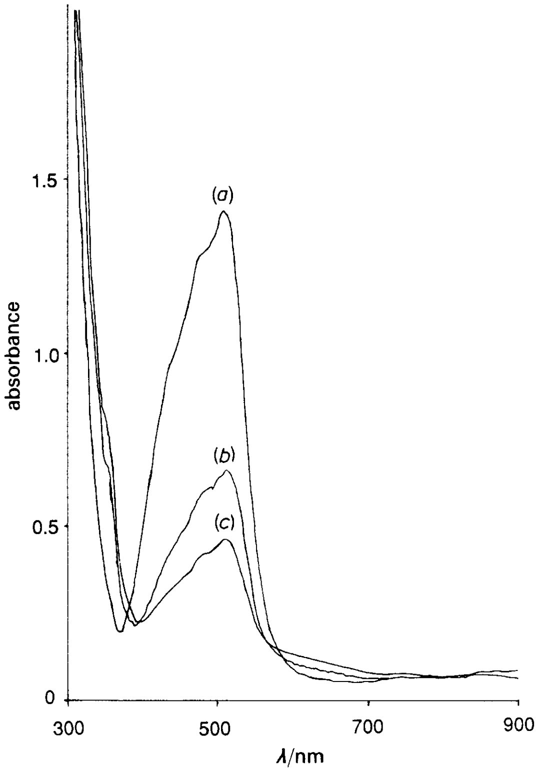

Fig. 2 Absorbance spectra of a series of solutions (2.5 cm^3, 0.5 mol dm^{-3} H_2SO_4), containing either: (*a*) an unchanged dispersion of $RuO_2 \cdot xH_2O$ (100 mg dm^{-3}), (*b*) 40 mm^3 of a 0.01 mol dm^{-3} Ce^{IV} solution or, (*c*) a charged dispersion of $RuO_2 \cdot xH_2O$ (100 mg dm^{-3}), to which ferroin has been added (80 mm^3, 0.005 mol dm^{-3}). In runs (*a*) and (*c*) the background absorbance spectrum due to the $RuO_2 \cdot xH_2O$ dispersion has been subtracted from the overall absorbance spectrum

The results of the redox indicator experiments contradict the simple idea of a water-soluble impurity reductant as the cause of these charging effects. In adddition, we have found that these results can be reproduced using highly hydrated $RuO_2 \cdot xH_2O$ from a number of different commercial sources or prepared by the alkaline hydrolysis plus aerobic oxidation of ruthenium trichloride; therefore, this phenomenon does not depend upon the source of the $RuO_2 \cdot xH_2O$ used. It might be argued that the oxidising nature of the charged $RuO_2 \cdot xH_2O$ particles is due to adsorbed Ce^{IV} ions; however, the bulk [Ce^{III}] can also be determined spectrophotometrically after the [Ce^{IV}] has dropped to $\leqslant 1\%$ of its initial value and the results indicate that no Ce^{IV} ions are adsorbed onto the $RuO_2 \cdot xH_2O$ particles, as might be

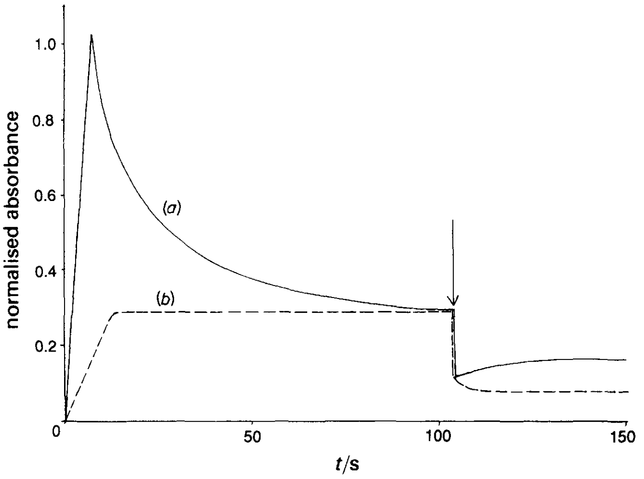

Fig. 3 Relative absorbance *vs.* time profiles recorded when first a solution of Ce^{IV} ions [(*a*) 50 mm^3, 0.01 mol dm^{-3}, or (*b*) 14 mm^3, 0.01 mol dm^{-3}] and then a solution of ferrous ions (10 mm^3, 0.01 mol dm^{-3}; addition denoted by the arrow) were added to 2.5 cm^3 of a dispersion of $RuO_2 \cdot xH_2O$ (100 mg dm^{-3}) in 0.5 mol dm^{-3} H_2SO_4 containing an excess of Ce^{III} ions (0.074 mol dm^{-3})

expected given that the p.z.c. of $RuO_2 \cdot xH_2O$ is *ca.* 2.7 and the pH of our solutions in all our experiments (pH 0) is much less than this.

Further evidence for the charging mechanism comes from a very simple experiment in which Fe^{II} ions (10 mm^3, 0.01 mol dm^{-3}) are injected into a charged dispersion (2.5 cm^3) of $RuO_2 \cdot xH_2O$ (100 mg dm^{-3}) with an excess of Ce^{III} ions (0.074 mol dm^{-3}). The results of such an experiment are illustrated in Fig. 3(*a*), along with a blank run (*i.e.* no $RuO_2 \cdot xH_2O$ present), Fig. 3(*b*). The charging model provides a ready explanation for the observed absorbance *vs.* time profile in Fig. 3(*a*), *i.e.* with the addition of Ce^{IV} ions (50 mm^3, 0.01 mol dm^{-3}) some decay in the initial [Ce^{IV}] occurs owing to charging of the $RuO_2 \cdot xH_2O$ particles (note that it is only a partial decay because there is a high background concentration of Ce^{III} ions) and this process of charging slows down as the potential on the $RuO_2 \cdot xH_2O$ particles reaches that of the bulk solution (E_1). Addition of Fe^{II} ions to the charged dispersion (indicated in Fig. 3 by the arrow) results in the rapid homogeneous reduction of Ce^{IV} ions in the bulk solution, thereby causing the potential of the bulk solution to drop to E_2 (where $E_1 > E_2$). However, this leaves $RuO_2 \cdot xH_2O$ particles 'over-charged', *i.e.* at a potential E_1, since the heterogeneous reduction of the charge $RuO_2 \cdot xH_2O$ particles by Fe^{II} ions is likely to be much slower than the homogeneous reaction with Ce^{IV} ions. As a result, after the fast initial drop in [Ce^{IV}], following the injection of Fe^{II} ions, there is a subsequent slow reoxidation of some Ce^{III} to Ce^{IV} by the over-charged $RuO_2 \cdot xH_2O$ particles until the potential of both the particles and bulk solution are the same. In the blank experiment [Fig. 3(*b*)] sufficient Ce^{IV} ions were injected to give the same [Ce^{IV}] as that of the $RuO_2 \cdot xH_2O$ dispersion experiment [see Fig. 3(*a*)] prior to injection of Fe^{II} ions. In contrast to the charged particle experiment [Fig. 3(*a*)], in the blank experiment the drop in [Ce^{IV}] is instantaneous and there is no evidence of any recovery in [Ce^{IV}], see Fig. 3(*b*).

The kinetics of the primary step, *i.e.* the charging step, in the dissolution of $RuO_2 \cdot xH_2O$ were studied as a function of [$RuO_2 \cdot xH_2O$] and temperature. In this work, typically, 50 mm^3 of a 0.01 mol dm^{-3} Ce^{IV} solution were injected into 2.5 cm^3 of a stock dispersion of $RuO_2 \cdot xH_2O$ (100 mg dm^{-3}) containing 0.074 mol dm^{-3} Ce^{III} ions. For every kinetic run the initial rate was determined from the computer-calculated derivative form of the recorded Ce^{IV} absorbance *vs.* time plot.

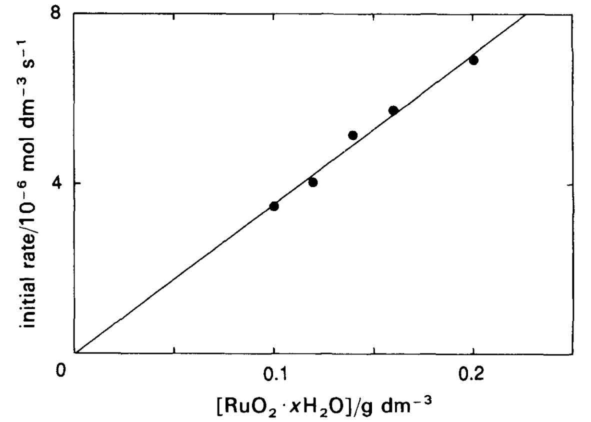

Fig. 4 Initial rate (/mol dm^{-3} s^{-1}) *vs.* [$RuO_2 \cdot xH_2O$]. In this work 50 mm^3 of a 0.01 mol dm^{-3} Ce^{IV} solution was injected into 2.5 cm^3 of the $RuO_2 \cdot xH_2O$ dispersion in 0.5 mol dm^{-3} H_2SO_4 and containing 0.074 mol dm^{-3} Ce^{III} ions

In this work the study of the effect of different concentrations of $RuO_2 \cdot xH_2O$ on the initial rate of Ce^{IV} reduction was limited, since the initial [$RuO_2 \cdot xH_2O$] must be significantly in excess with respect to the initial [Ce^{IV}] and the absorbance of the dispersion alone must be not be so high (*i.e.* >2, say) that their measurement is unreliable. As a consequence, [$RuO_2 \cdot xH_2O$] was varied over the limited range 100–200 mg dm^{-3} and the resulting plot of initial rate *vs.* [$RuO_2 \cdot xH_2O$] is illustrated in Fig. 4. From the data illustrated in Fig. 4, it appears that the initial rate of Ce^{IV} reduction is proportional to [$RuO_2 \cdot xH_2O$] and is zero at zero $RuO_2 \cdot xH_2O$ concentration, as might be expected if the process is associated with the charging of the $RuO_2 \cdot xH_2O$ particles.

The initial rate of the primary step was also studied as a function of temperature over the range 22–40 °C with a $RuO_2 \cdot xH_2O$ concentration of 100 mg dm^{-3} and with all other conditions as in Fig. 4. This study was limited in that at temperatures $\geqslant 40$ °C the solubility of the cerium(III) sulphate, present at a high concentration in solution, had decreased sufficiently that problems resulting from its partial precipitation were encountered. An Arrhenius plot of the data is illustrated in Fig. 5 and from a least-squares analysis of the data an activation energy of 25 ± 4 kJ mol^{-1} can be calcu-

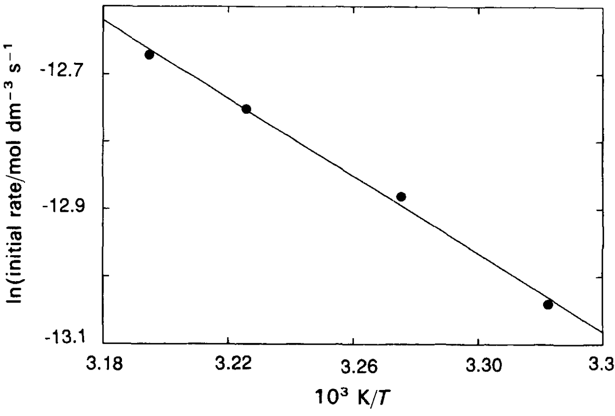

Fig. 5 Arrhenius plot of initial rate (/mol dm^3 s^{-1}) as a function of temperature (*T*), over the range 22–40 °C, for the charging process. In this work the reaction conditions were as described for Fig. 4, with [$RuO_2 \cdot xH_2O$] = 100 mg dm^{-3}. The solid line was that of best fit to the data as determined by the method of least squares

lated which compares favourably with the value range (15–19 kJ mol^{-1}) expected for a diffusion-controlled process such as charging.[16]

Experiments using Excess of Ce^{IV}

Previous work[6] has established that in the presence of excess of Ce^{IV} ions the dissolution of $RuO_2 \cdot xH_2O$ to RuO_4, with the concomitant generation of a small amount of O_2, has the reaction stoichiometry indicated in reactions (2*a*) and (2*b*), *i.e.* there is no evidence of charging. However, if dissolution proceeds *via* an electrochemical mechanism some charging must precede particle dissolution. The process of charging is, as we have seen, most readily observed when the $[Ce^{IV}] : [RuO_2 \cdot xH_2O]$ ratio is very low (typically 0.35 : 1 in the previous experiments) and there is a high background concentration of Ce^{III} ions which impedes the subsequent dissolution process. In contrast, if $[RuO_2 \cdot xH_2O]$ is low and Ce^{IV} ions are in excess, *i.e.* typically with a $[Ce^{IV}] : [RuO_2 \cdot H_2O]$ ratio of 9 : 1, it has been established that the reduction of Ce^{IV} ions is almost wholly associated with the dissolution of $RuO_2 \cdot xH_2O$to RuO_4.

In a series of kinetic runs 90 mm^3 of a 0.1 mol dm^{-3} Ce^{IV} solution were injected into a dispersion of $RuO_2 \cdot xH_2O$ (2.72 cm^3, 51 mg dm^{-3}) containing different concentrations of Ce^{III} ions, ranging from to 0 to 0.074 mol dm^{-3}. Fig. 6 illustrates a selection of the absorbance *vs.* time profiles generated from this work, from which it is clear that the rate of dissolution decreases with increasing $[Ce^{III}]$. In a previous paper[11] we investigated the kinetics of water oxidation by Ce^{IV} ions mediated by thermally activated ruthenium dioxide hydrate and found that the reaction was also inhibited by Ce^{III} ions. The kinetics of this redox-catalysed process were readily rationalised in terms of an electrochemical model in which the reduction of Ce^{IV} ions and oxidation of water were taken as highly reversible and irreversible reactions, respectively.[12] These two redox processes were coupled together *via* the particles of thermally activated ruthenium dioxide hydrate, which acted as microelectrodes poised at a 'mixture potential', E_{mix}, and providing a medium through which electrons were transferred from water to Ce^{IV}.

The dissolution of $RuO_2 \cdot xH_2O$ by Ce^{IV} ions may take place *via* a similar electrochemical mechanism in which the reduction of Ce^{IV} ions and oxidation of $RuO_2 \cdot xH_2O$ are assumed to be, respectively, highly reversible and irreversible processes, with the particles of $RuO_2 \cdot xH_2O$ acting as dissolving microelectrodes. Under these circumstances the cathodic current ($i_{c,t}$) due to the reduction of Ce^{IV} ions, at any time *t* during the dissolution process, will be related to $[Ce^{IV}]_t$, $[Ce^{III}]_t$ and$E_{mix,t}$ *via* the expression.[11,12]

$$-i_{c,t} = \frac{k_d F A_t\{[Ce^{IV}]_t - [Ce^{III}]_t \exp[F(E_{mix,t} - E_{Ce})/RT]\}}{1 + \exp[F(E_{mix,t} - E_{Ce})/RT]} \qquad \text{(I)}$$

where A_t is the total surface area of the $RuO_2 \cdot xH_2O$ particles at time *t*, k_d is the mass-transfer coefficient for Ce^{IV} and Ce^{III} ions and E_{Ce} is the formal redox potential of the Ce^{IV}/Ce^{III} couple (taken as 1.44 V *vs.* NHE). We can see from eqn. (I) that the rate (which is proportional to $i_{c,t}$) will decrease as the initial $[Ce^{III}]$ is increased, which is in qualitative agreement with the absorbance due to Ce^{IV} ions $[A(Ce^{IV})]$ *vs.* time decay profiles illustrated in Fig. 6.

In our work, in any kinetic run an $A(Ce^{IV})$ *vs.* time profile is recorded for the reduction of Ce^{IV} ions from which the cathodic current at any time *t* can be calculated using the derivative, $dA(Ce^{IV})/dt = \Delta_t$ (a measurable quantity) and the expression:

$$i_{c,t} = KF\Delta_t \qquad \text{(II)}$$

where *K* is a proportionality constant equal to $1/[\varepsilon(Ce^{IV})_{430} l]$, with $\varepsilon(Ce^{IV})_{430} = 290$ dm^3 mol^{-1} cm^{-1} and $l = 1$ cm (cell pathlength). If the concentration of Ce^{III} ions is very low, *e.g.* in the absence of any initial Ce^{III} ions and at or near to the beginning of the dissolution process, the combination of eqn. (I) and (II) simplifies to

$$i_{c,t} = -k_d F A_t [Ce^{4+}]_t = KF\Delta_{t'} \qquad \text{(III)}$$

Under these conditions the current is diffusion-controlled and thus the derivative has a maximum value, $\Delta_{t'}$, for a given total surface area of A_t.

Eqn. (I)–(III) can be combined to generate the following useful expression for the mixture potential on the $RuO_2 \cdot xH_2O$ particles at time *t* and surface area A_t

$$E_{mix,t} = E_{Ce} + RT/F \ln\{(\Delta_{t'} - \Delta_t)/(\Delta_t + \Delta_{t'}[Ce^{III}]_t/[Ce^{IV}]_t)\} \qquad \text{(IV)}$$

In our work the rate of reduction of the Ce^{IV} ions was studied as a function of $[Ce^{III}]$, *e.g.* see Fig. 6. In order to fix A_t, albeit at some unknown value, the initial concentrations of Ce^{IV} ions and $RuO_2 \cdot xH_2O$ were themselves fixed and, from the absorbance *vs.* time profiles, the derivative, Δ_t, was determined as a function of $[Ce^{III}]$ after a set fraction (5%) of the overall drop in $[Ce^{IV}]$ had occurred. (Note that $\Delta_{t'}$ was taken as the value of Δ_t for the kinetic run with an initial $[Ce^{III}]$ of 0 mol dm^{-3}, *i.e.* Fig. 6(*a*). Thus, given these conditions, the values of $i_{c,t}$ and $E_{mix,t}$ were determined for each kinetic run, after 5% dissolution, using eqn. (III) and (IV), respectively.

If the dissolution of $RuO_2 \cdot xH_2O$ is a highly irreversible reaction, as we have assumed, then the corrosion current will be related to the mixture potential on the $RuO_2 \cdot xH_2O$ particles *via* the expresssion:

$$i_{corr} = i_0 \exp(2.303\eta/b) \qquad \text{(V)}$$

where, i_0 is the exchange current for the $RuO_2 \cdot xH_2O/RuO_4$ couple, *b* is the Tafel slope and η is the difference between $E_{mix,t}$ and the equilibrium potential for the $RuO_2 \cdot xH_2O/RuO_4$ couple. If the Wagner–Traud additivity principle applies, the net current of the system is zero, *i.e.*

$$i_{corr} = -i_{c,t} = i_{mix,t} \qquad \text{(VI)}$$

Thus, it follows that a major prediction of our electrochemical model for the dissolution of $RuO_2 \cdot xH_2O$ by Ce^{IV} ions is that a plot of $E_{mix,t}$ *vs.* $\log(\Delta_t)$ [which is proportional to $\log(i_{mix,t})$] should be a straight line of gradient *b*.

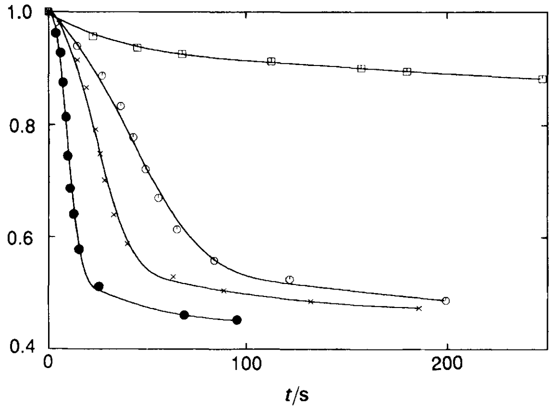

Fig. 6 Relative absorbance *vs.* time profiles for the dissolution reaction when an excess of Ce^{IV} ions (90 mm^3, 0.1 mol dm^{-3}) was injected into 2.72 cm^3 of a dispersion of $RuO_2 \cdot xH_2O$ (51 mg dm^{-3}) in 0.5 mol dm^{-3} H_2SO_4 containing: ●, 0.0; ×, 0.0064; ○, 0.0096; □, 0.0256 mol dm^{-3} Ce^{III} ions

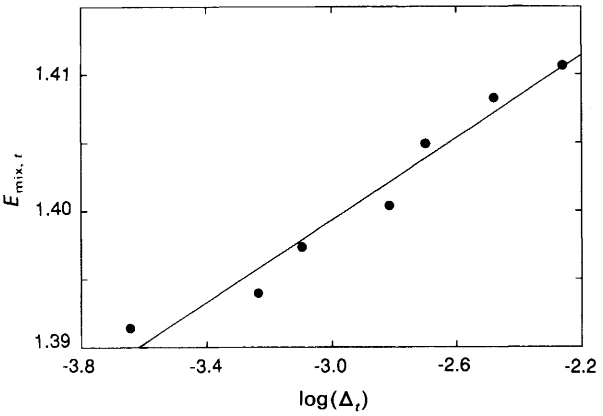

Fig. 7 Tafel plot of $E_{mix,t}$ vs. log(Δ_t), where $\Delta_t = \mathrm{d}\,A(\mathrm{Ce^{IV}})_{430}/\mathrm{d}t$ after 5% of the overall reaction has occurred. The values for Δ_t were determined from a series of absorbance vs. time profiles recorded in the presence of different amounts of excess $\mathrm{Ce^{IV}}$ ions, some of which are illustrated in Fig. 6.

From an analysis of the results of our series of kinetic runs in which the initial concentration of $\mathrm{Ce^{III}}$ was varied (see Fig. 7) this prediction appears to be confirmed, since a plot of $E_{mix,t}$ vs. log(Δ_t) is a reasonable straight line with a gradient of 15 ± 1 mV per decade, as illustrated in Fig. 7. The Tafel slope of 15 mV per decade may be rationalised in terms of a mechanism which is similar to that of the 'oxide pathway' for water oxidation,[17] *i.e.*

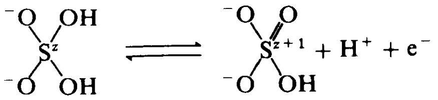
(5)

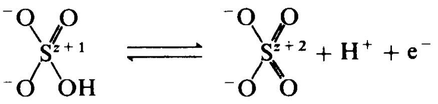
(6)

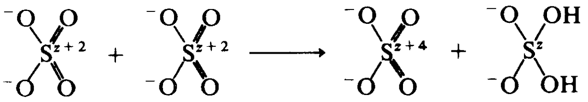
(7)

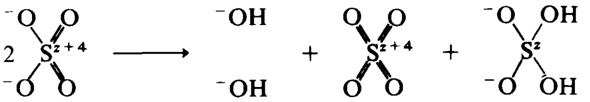
(8)

where S^z is $\mathrm{Ru^{IV}}$. There is work[3] to suggest that the corrosion of RuO_2 electrodes involves the same types of active surface group as involved in the oxidation of water and that a highly reactive $\mathrm{Ru^{VIII}}$ surface species is a precursor to both water oxidation and $RuO_2 \cdot xH_2O$ dissolution [see reaction (8)]. Central to the ability of RuO_2 to resist corrosion and promote water oxidation, which $RuO_2 \cdot xH_2O$ lacks, is the stability of this surface $\mathrm{Ru^{VIII}}$ species; clearly in $RuO_2 \cdot xH_2O$ the $\mathrm{Ru^{VIII}}$ species generated is unstable and prone to dissolution. It can be shown that if reaction (7) is rate-limiting and surface coverage by the intermediates involved is low, then the Tafel slope will be 15 mV per decade, as appears to be the case in our work for the $RuO_2 \cdot xH_2O$ microelectrode particles (see Fig. 7).

In another set of experiments the kinetics of $RuO_2 \cdot xH_2O$ dissolution by $\mathrm{Ce^{IV}}$ ions were studied as a function of temperature. In this work, Δ_t (after 5% reaction) was determined as a function of temperature over the range 15–25 °C with an initial [$\mathrm{Ce^{III}}$] of 0 mol dm^{-3}. In the absence of a high initial [$\mathrm{Ce^{III}}$] the electrochemical model predicts that the rate of reduction of $\mathrm{Ce^{IV}}$ ions should be diffusion-controlled [see eqn. (III)]. From the Arrhenius plot of the results [*i.e.* ln(Δ_t) vs. $1/T$] an activation energy of 23 ± 4 kJ mol^{-1} was calculated, which compares favourably with that expected for a diffusion-controlled reaction.

In the presence of a high initial concentration of $\mathrm{Ce^{III}}$ ions the electrochemical model predicts that the reaction will not be diffusion-controlled, but, instead, will reflect the activation energy for the dissolution of $RuO_2 \cdot xH_2O$ to RuO_4. In a second set of experiments, Δ_t (after 5% reaction) was determined as a function of temperature using the same conditions as before, but in the presence of 1.7×10^{-2} mol dm^{-3} $\mathrm{Ce^{III}}$ ions ([$\mathrm{Ce^{IV}}$] : [$\mathrm{Ce^{III}}$] = 1 : 5). From the slope of an Arrhenius plot of the results an activation energy of 39 ± 5 kJ mol^{-1} was calculated.

Conclusions

The kinetics of oxidative dissolution of $RuO_2 \cdot xH_2O$ to RuO_4 by $\mathrm{Ce^{IV}}$ ions appear to obey an electrochemical mechanism in which the $RuO_2 \cdot xH_2O$ particles are charged up prior to dissolution. The process of charging, rather than of $RuO_2 \cdot xH_2O$ dissolution, appears to be dominant if the [$\mathrm{Ce^{IV}}$] : [$RuO_2 \cdot xH_2O$] ratio is low (*e.g.* 0.35 : 1) and the background concentration of $\mathrm{Ce^{III}}$ ions is also high. In contrast, dissolution is the dominant process when the [$\mathrm{Ce^{IV}}$] : [$RuO_2 \cdot xH_2O$] ratio is high (*e.g.* 9 : 1) and the background [$\mathrm{Ce^{III}}$] low. The kinetics of dissolution fit an electrochemical model in which the reduction of $\mathrm{Ce^{IV}}$ ions and the oxidation of $RuO_2 \cdot xH_2O$ to RuO_4 are assumed to be highly reversible and irreversible processes, respectively, mediated by the dissolving microelectrode particles of $RuO_2 \cdot xH_2O$. Assuming this electrochemical model, from an analysis of the kinetics of dissolution the Tafel slope for the corrosion of $RuO_2 \cdot xH_2O$ was calculated as 15 mV per decade, and the activation energy was estimated to be 39 ± 5 kJ mol^{-1}.

We thank the SERC for supporting this work.

References

1 *Electrodes of Conductive Metallic Oxides*, ed. S. Trasatti, Elsevier, Amsterdam, 1980, parts A and B.
2 C. Iwakura, K. Hirao and H. Tamura, *Electrochim. Acta*, 1977, **22**, 329.
3 H. J. Lewrenz, S. Stuki and R. Kötz, *Surf. Sci.*, 1983, **126**, 463.
4 A. Mills, *Chem. Soc. Rev.*, 1989, **18**, 285, and references therein.
5 A. Mills, S. Giddings, I. Patel and C. Lawrence, *J. Chem. Soc., Faraday Trans. 1*, 1987, **83**, 2331.
6 A. Mills, S. Giddings and I. Patel, *J. Chem. Soc., Faraday Trans. 1*, 1987, **83**, 2317.
7 R. Mason, A. Mills and D. Milton, *J. Less-Common Met.*, 1989, **155**, 89.
8 M. Spiro, *Chem. Soc. Rev.*, 1986, **15**, 141.
9 *Electrochemical Techniques for Corrosion*, ed. R. Baboian, N.A.C.E., Katy, Texas, 1977.
10 M. G. Segal and R. M. Sellers, *Adv. Inorg. Bioinorg. Mech.*, 1984, **3**, 97, and references therein.
11 A. Mills and N. McMurray, *J. Chem. Soc., Faraday Trans. 1*, 1989, **85**, 2055.
12 A. Mills and N. McMurray, *J. Chem. Soc., Faraday Trans. 1*, 1989, **85**, 2047.
13 A. Mills and S. Giddings, *J. Org. Chem.*, 1988, **53**, 1103.
14 A. Mills, S. Giddings, N. McMurray and G. Williams, *Inorg. Chim. Acta*, 1989, **159**, 7.
15 A. Henglein, *J. Phys. Chem.*, 1979, **83**, 2209.
16 F. Wilkinson, *Chemical Kinetics and Reaction Mechanism*, Van Nostrand Reinhold, London, 1981, p. 140.
17 J. O'M. Bockris, *J. Chem. Phys.*, 1956, **24**, 817.

Paper 0/03037F; *Received* 6th *July*, 1990